



**HAL**  
open science

## The absence of telomerase leads to immune response and tumor regression in zebrafish melanoma

Bruno Lopes-Bastos, Joana Nabais, Tânia Ferreira, Giulia Allavena, Mounir El Maï, Malia Bird, Seniye Targen, Lorenzo Tattini, Da Kang, Jia-Xing Yue,  
et al.

### ► To cite this version:

Bruno Lopes-Bastos, Joana Nabais, Tânia Ferreira, Giulia Allavena, Mounir El Maï, et al.. The absence of telomerase leads to immune response and tumor regression in zebrafish melanoma. *Cell Reports*, 2024, 43 (12), pp.115035. 10.1016/j.celrep.2024.115035 . hal-04820218

HAL Id: hal-04820218

<https://hal.science/hal-04820218v1>

Submitted on 5 Dec 2024

**HAL** is a multi-disciplinary open access archive for the deposit and dissemination of scientific research documents, whether they are published or not. The documents may come from teaching and research institutions in France or abroad, or from public or private research centers.

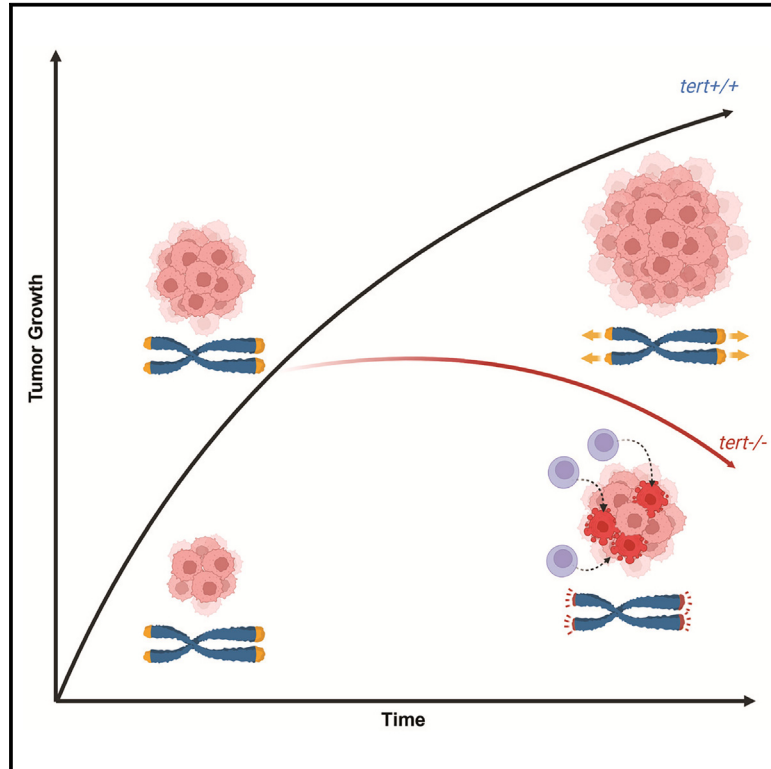
L'archive ouverte pluridisciplinaire **HAL**, est destinée au dépôt et à la diffusion de documents scientifiques de niveau recherche, publiés ou non, émanant des établissements d'enseignement et de recherche français ou étrangers, des laboratoires publics ou privés.



Distributed under a Creative Commons Attribution - NonCommercial 4.0 International License

# The absence of telomerase leads to immune response and tumor regression in zebrafish melanoma

## Graphical abstract



## Authors

Bruno Lopes-Bastos, Joana Nabais, Tânia Ferreira, ..., Gianni Liti, Tânia G. Carvalho, Miguel Godinho Ferreira

## Correspondence

miguel-godinho.ferreira@unice.fr

## In brief

Lopes-Bastos et al. report that melanoma in zebrafish initiates without telomerase (or ALT) activation. However, in late progression, telomerase becomes essential for sustained tumor growth. Tumors that fail to re-activate telomerase slow down growth and even regress. This occurs due to tumor-autonomous (genomic instability) and non-tumor-autonomous (immune response) mechanisms.

## Highlights

- Melanoma initiation and early progression occur without the need for telomerase (or ALT)
- Telomerase re-activation is crucial for sustained tumor growth at later stages
- Lack of telomerase leads to tumor regression via genome instability and immune response
- Nevertheless, telomerase-negative melanomas remain aggressive and lethal



## Article

# The absence of telomerase leads to immune response and tumor regression in zebrafish melanoma

Bruno Lopes-Bastos,<sup>1,2</sup> Joana Nabais,<sup>2</sup> Tânia Ferreira,<sup>2</sup> Giulia Allavena,<sup>1</sup> Mounir El Maï,<sup>1,2</sup> Malia Bird,<sup>1</sup> Seniye Targen,<sup>1</sup> Lorenzo Tattini,<sup>1</sup> Da Kang,<sup>3</sup> Jia-Xing Yue,<sup>3</sup> Gianni Liti,<sup>1</sup> Tânia G. Carvalho,<sup>4</sup> and Miguel Godinho Ferreira<sup>1,2,5,\*</sup>

<sup>1</sup>Institute for Research on Cancer and Aging of Nice (IRCAN), CNRS UMR7284, INSERM U1081, Université Côte d'Azur, 06107 Nice, France

<sup>2</sup>Instituto Gulbenkian de Ciência, 2780-156 Oeiras, Portugal

<sup>3</sup>State Key Laboratory of Oncology in South China, Collaborative Innovation Center for Cancer Medicine, Sun Yat-sen University Cancer Center, Guangzhou, China

<sup>4</sup>Champalimaud Center for the Unknown, 1400-038 Lisboa, Portugal

<sup>5</sup>Lead contact

\*Correspondence: [miguel-godinho.ferreira@unice.fr](mailto:miguel-godinho.ferreira@unice.fr)

<https://doi.org/10.1016/j.celrep.2024.115035>

## SUMMARY

Most cancers re-activate telomerase to maintain telomere length and thus acquire immortality. Activating telomerase promoter mutations are found in many cancers, including melanoma. However, it is unclear when and if telomerase is strictly required during tumorigenesis. We combined the telomerase mutant (*tert*<sup>-/-</sup>) with two established zebrafish melanoma models. We show that *tert*<sup>-/-</sup> melanomas initially develop with similar incidence and invasiveness to *tert*<sup>+/+</sup> tumors. However, they eventually decline in growth and regress. Late *tert*<sup>-/-</sup> tumors exhibit reduced cell proliferation, increased apoptosis, and melanocyte differentiation. Notably, these tumors show enhanced immune cell infiltration and can resume growth when transplanted into immunocompromised hosts. We propose that telomerase is required for melanoma in zebrafish, albeit at later stages of progression, to sustain tumor growth while avoiding immune rejection and regression. Thus, the absence of telomerase restricts melanoma through tumor-autonomous mechanisms (cell-cycle arrest, apoptosis, and melanocyte differentiation) and a non-tumor-autonomous mechanism (immune rejection).

## INTRODUCTION

In most adult somatic tissues, telomeres shorten through successive cell divisions. Short telomeres cause telomere dysfunction, leading to replicative senescence and cell-cycle arrest.<sup>1–4</sup> Telomere shortening imposes two proliferation barriers that pre-cancerous cells must overcome to become fully malignant.<sup>5,6</sup> The first proliferation barrier, known as M1 or senescence, is composed of a p53-dependent mechanism, which can be overcome by the loss of p53/Rb function. The second, known as M2 or crisis, is characterized by increased genome instability fueled by telomere-to-telomere fusions.<sup>5</sup> To reverse this state, cells must engage in a telomere maintenance mechanism (TMM). Approximately 90% of human tumors re-activate telomerase, thus elongating telomeres and chromosome-end protection.<sup>7</sup> Telomerase is composed of two core components, a reverse transcriptase DNA polymerase subunit (TERT) and a template containing a noncoding RNA subunit (TR). Telomerase binds to the 3' end of telomeres and processively adds (TTAGGG)<sub>n</sub> hexanucleotide repeats.<sup>8</sup> In the absence of telomerase, cancer cells can maintain telomeres through a recombination-based mechanism known as alternative lengthening of telomeres (ALT).<sup>6,9</sup> *In vivo* studies using murine models showed that the lack of telomerase, in animals with short telomeres, results in less cancer formation.<sup>10,11</sup> Additionally, telomerase inhibition of established tumors resulted in growth restriction.<sup>10</sup> Interestingly, tumor relapse upon telomerase inhibition was observed in some animals in which ALT was detected,<sup>10</sup> showing that ALT can be an efficient TMM in tumorigenesis. ALT was also observed in zebrafish brain tumors.<sup>12</sup>

In contrast to the previous idea, a study that analyzed 31 cancer types failed to detect TMMs in 22% of 6,835 human samples.<sup>13</sup> In addition, tissue culture of cells derived from melanoma and neuroblastoma TERT-/ALT- tumors displayed progressive telomere shortening, confirming those tumors lacked an active TMM in patients.<sup>14,15</sup> Cancers lacking TMMs come at a cost that limits their replicative capacity imposed by the Hayflick limit. This trade-off is illustrated by neuroblastoma lacking TMMs. These cancers present a better prognosis and are correlated with spontaneous regression.<sup>16</sup> However, this is not always the case. Melanomas lacking a TMM were reported to be extremely aggressive, despite limited proliferative capacity in cell culture.<sup>15</sup> In addition, TMMs may play a role in resistance to immunotherapies. Studies have shown that metastatic melanoma resistant

to immunotherapies. Studies have shown that metastatic melanoma resistant



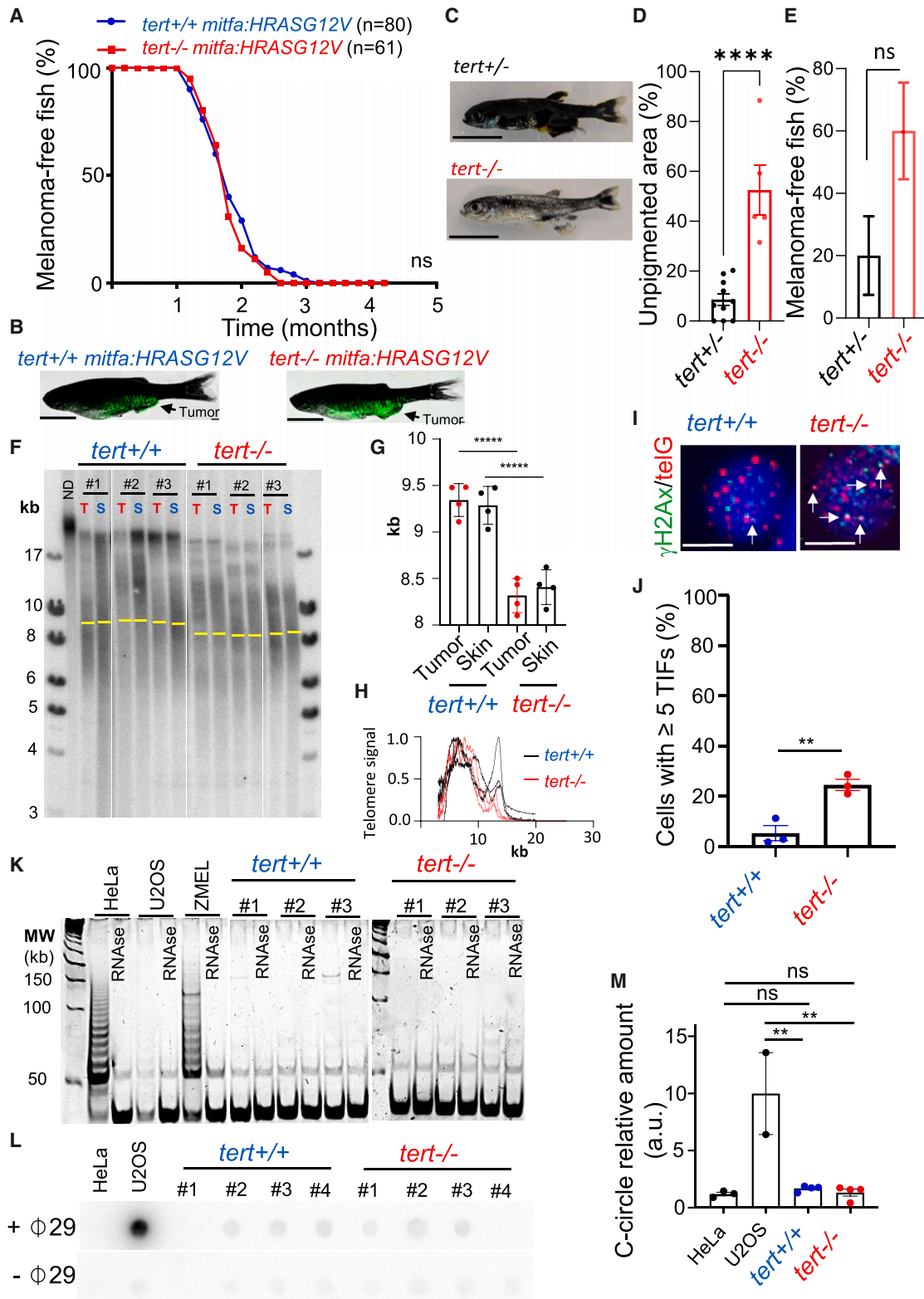


**Figure 1. Melanoma initiation does not require a telomere maintenance mechanism**

(A and B) Incidence of melanoma of *mitfa:HRAS* fish is not affected by the lack of telomerase. (A) Percentage of tumor-free fish compared between *tert*<sup>+/+</sup> and *tert*<sup>-/-</sup> fish (log rank test). (B) Representative images of 3-month-old *tert*<sup>+/+</sup> and *tert*<sup>-/-</sup> fish with melanoma expressing GFP. Scale bars: 0.5 cm.

(legend continued on next page)

to immune checkpoint blockade therapies displays an increased expression of genes related to telomere maintenance,<sup>17</sup> while TERT mutations can predict the response to some immune checkpoint blockade therapies.<sup>18,19</sup> These findings suggest that telomerase expression may regulate cancer immunogenicity, potentially serving as a predictive biomarker for therapy.

Replicative immortality provided by TMMs is a well-established hallmark of cancer. However, it is unclear when during tumorigenesis TMMs become activated and whether they are strictly essential for lethal cancers. Activating TERT promoter mutations (TPMs) are found at a high frequency in several human tumor types.<sup>20–23</sup> These tumors include cutaneous melanomas at a frequency of 60%–85%.<sup>20,21,24</sup> TPMs have been identified in both early- and late-stage tumors,<sup>20–23,25</sup> suggesting that telomerase activation may occur throughout tumorigenesis. Here, we investigated the role of telomerase in melanoma initiation and progression with the goal of identifying at which stage TMMs are strictly required for tumorigenesis. Unexpectedly, we observed that melanoma initiation and early progression do not require telomerase or ALT. However, the lack of telomerase activity at later stages restricted melanoma growth and led to tumor regression through both tumor-autonomous and non-tumor-autonomous mechanisms.

## RESULTS

### Melanoma initiation and early progression do not require TMMs

To determine the role of telomerase in melanoma, we crossed the telomerase mutant zebrafish (*tert*<sup>hu3430/hu3430</sup>, hereby referred as *tert*<sup>-/-</sup>), in which telomerase is enzymatically inactive,<sup>26</sup> with the *Tg(mitfa:Hsa.HRAS\_G12V,mitfa:GFP)* melanoma model, referred to here as *mitfa:HRAS*, developed by the Hurlstone lab.<sup>27</sup> Melanocytes of *mitfa:HRAS* fish were shown to exhibit hyperplasia, dysplasia, and spontaneous progression to invasive melanoma.<sup>27</sup> In agreement, we observe that wild-type (WT) telomerase (*tert*<sup>+/+</sup>) developed melanoma, reaching full penetrance by 4 months of age (Figure 1A). In this model, the transgene also induces the expression of GFP under the *mitfa* promoter to identify tumor development (Figure 1B). Surprisingly, the lack of telomerase activity in telomerase mutant fish harboring *mitfa:HRAS* (*mitfa:HRAS; tert*<sup>-/-</sup>) did not affect the dynamics of melanoma incidence (Figure 1A). Thus, telomerase is not

required for melanoma formation in this model. This result differs from previous data indicating that late-generation telomerase-deficient mice (G5 *Terc*<sup>-/-</sup>) are resistant to skin carcinoma.<sup>11</sup>

To extend our findings, we combined the telomerase mutant fish with a second widely used melanoma model expressing the human *BRAF*<sup>V600E</sup> oncogene in a *tp53*-deficient background, *Tg(mitfa:BRAF<sup>V600E</sup>); tp53<sup>-/-</sup>*.<sup>28</sup> Similarly, we observed that *Tg(mitfa:BRAF<sup>V600E</sup>); tp53<sup>-/-</sup>; tert<sup>-/-</sup>* does not affect melanoma incidence (Figure S1A). This second melanoma model also allowed us to observe the different phases of melanogenesis. In both *tert*<sup>+/+</sup> and *tert*<sup>-/-</sup>, we observed the three different stages of melanoma progression: benign lesion, radial growth phase, and vertical growth phase (Figure S1B). Our results show that even in the absence of telomerase, melanoma progresses efficiently through all these stages. Even though *BRAFV600E* is the most frequent alteration in melanoma, we chose to conduct our remaining experiments using the *mitfa:HRAS* melanoma model. In contrast to the *mitfa:BRAF<sup>V600E</sup>* model, the *mitfa:HRAS* zebrafish do not require a pre-existing *tp53* mutation to develop tumors.<sup>27</sup> We and others have shown that p53 dysfunction suppresses *tert*<sup>-/-</sup>, and *tert*<sup>-/-</sup> *tp53*<sup>-/-</sup> double mutants do not display the phenotypes associated with a lack of telomerase.<sup>26,29</sup> Therefore, the *mitfa:BRAF<sup>V600E</sup>* model would not allow us to directly investigate the function of telomerase in tumorigenesis. It is worth noting that Ras mutations, albeit less frequent, are still present in human melanoma and in need of effective therapies.<sup>24</sup>

In order to evaluate whether telomerase has an impact on melanoma initiation, we studied the incidence of early tumorigenesis in *mitfa:HRAS; tert*<sup>-/-</sup> fish. Our results show that a lack of telomerase did not affect either the development of microtumors in 1- to 2-month-old fish (Figures S1C and S1D) or their invasiveness capacity (Figures S1E and S1F). The similar incidence of early tumors in telomerase mutant fish reinforces the idea that telomerase activation is not required for cancer initiation.

Once the experimental fish were generated by a *tert*<sup>+/-</sup> in-cross, another explanation for why *tert*<sup>-/-</sup> fish develop tumors could be the presence of maternal *tert* mRNA, allowing melanocytes to elongate their telomeres during development. To test this hypothesis, we crossed a *tert*<sup>-/-</sup> female with a *tert*<sup>+/-</sup> male, producing a mix of *tert*<sup>+/-</sup> and *tert*<sup>-/-</sup> progeny. This setup is not ideal, as the offspring will inherit the very short telomeres of *tert*<sup>-/-</sup> females. We observed a reduction in the number of

(C–E) *tert* mRNA maternal contribution does not explain carcinogenesis in *tert*<sup>-/-</sup> fish. (C and D) Representative images and quantification of unpigmented skin area of *mitfa:HRAS:GFP*, *tert*<sup>+/-</sup> and *tert*<sup>-/-</sup> fish at 1.5 months of age.  $n(\textit{tert}^{+/-}) = 10$ ;  $\textit{tert}^{-/-} = 5$ ; unpaired t test. Scale bars: 0.5 cm. (E) Quantification of fish with tumors at 1.5 months of age.  $n(\textit{tert}^{+/-}) = 10$ ;  $\textit{tert}^{-/-} = 5$ ;  $\chi^2$  test.

(F–H) Even though telomere shortening is not apparent between skin and tumor in *tert*<sup>-/-</sup> fish, there is telomere shortening in *tert*<sup>-/-</sup> skin/tumor when compared to *tert*<sup>+/-</sup> fish. However, *tert*<sup>-/-</sup> tumors possess higher DNA damage at telomeres. (F) Telomere restriction fragment (TRF) analysis by Southern blotting of tumor (T) and skin (S) genomic DNA extracted from 3-month-old fish (yellow bars represent mean telomere length) and (G) quantifications for mean telomere length and (H) densitometries of TRFs ( $n = 4$ ; one-way ANOVA).

(I) Images of  $\gamma$ H2Ax/telG immunofluorescence *in situ* hybridization (immune-FISH) of tumor cells derived from *tert*<sup>+/-</sup> and *tert*<sup>-/-</sup> 3-month-old fish. White arrows indicate telomere dysfunction-induction foci (TIFs) in tumor cells. Scale bars: 6  $\mu$ m.

(J) Percentage of cells containing  $\geq 5$  TIFs from (I) ( $n = 3$ ; unpaired t test).

(K–M) Early-stage melanoma do not display TMMs. (K) Telomerase activity evaluated by TRAP of tumor samples derived from *tert*<sup>+/-</sup> and *tert*<sup>-/-</sup> 3-month-old fish ( $n = 3$ ). Extracts from HeLa and ZMEL cells were used as positive controls and U2OS as a negative control. (L) C-circle assay of tumor samples derived from *tert*<sup>+/-</sup> and *tert*<sup>-/-</sup> 3-month-old fish. Extracts from HeLa cells and U2OS were used as negative and positive controls, respectively. (M) Quantification of C-circle signal ( $n = 4$ ; one-way ANOVA).

Error bars represent  $\pm$  SEM; each dot represents an individual tumor; \*\* $p \leq 0.01$  and \*\*\*\* $p \leq 0.0001$ . ns, not significant.

*tert*<sup>-/-</sup> fish by 1.5 months of age compared to *tert*<sup>+/-</sup> (Figure S2A), even though the expected ratios for the two genotypes are 50% each. We also documented high mortality in *tert*<sup>-/-</sup> fish in the following month (Figure S2B;  $p = 0.000073$ ). This suggests that a cross between a *tert*<sup>-/-</sup> female and a *tert*<sup>+/-</sup> male results in *tert*<sup>-/-</sup> offspring with a more severe phenotype than those resulting from a *tert*<sup>+/-</sup> intercross (Figure S2C). Additionally, the resulting *tert*<sup>-/-</sup> fish exhibited significantly reduced skin pigmentation (Figures 1C and 1D;  $p < 0.0001$ ). Despite these phenotypes, 40% of the *tert*<sup>-/-</sup> fish developed tumors as early as 1.5 months (Figures 1E,  $p = 0.332922$ , and S2D), indicating that lethal melanoma can develop in absence of telomerase. Remarkably, the only *tert*<sup>-/-</sup> fish that survived to the end of the experiment showed continued tumor growth between 1.5 and 2.5 months (Figures S2E and S2F). This experiment reinforces our previous findings that telomerase is not required for tumor initiation and growth in zebrafish.

Next, we analyzed visible tumors of 3-month-old fish. We defined this age as an early progression stage in tumorigenesis given that almost all fish carry macroscopic lesions (Figure 1A). We measured telomere length using telomere restriction fragment (TRF) Southern blotting and compared telomeres from tumor samples to those derived from the skin of the same fish as internal controls. Consistent with our previous results, telomeres of *tert*<sup>-/-</sup> fish are shorter than *tert*<sup>+/+</sup> (Figures 1F and 1G). Unexpectedly, we failed to detect telomere shortening in tumors compared to skin from either *tert*<sup>+/+</sup> or *tert*<sup>-/-</sup> 3-month-old fish (Figures 1F and 1G). Nevertheless, *tert*<sup>-/-</sup> melanoma cells exhibited a significant increase in telomere damage-induced foci (TIFs) compared to *tert*<sup>+/+</sup> tumor cells (*tert*<sup>+/+</sup>: 5% versus *tert*<sup>-/-</sup>: 25%;  $n = 3$   $p = 0.0068$ ; Figures 1I and 1J). Thus, even though *tert*<sup>-/-</sup> melanomas show similar average telomere lengths compared to skin, our result show that *tert*<sup>-/-</sup> melanoma cells harbor critically short telomeres even at this early progression stage.

Most cancers present activating telomerase promoter mutations from the early stages of carcinogenesis.<sup>30</sup> To evaluate whether tumors in our model present telomerase activity, we performed a telomerase repeat amplification protocol (TRAP) assay. We used human HeLa cells and the zebrafish melanoma ZMEL cell line as positive controls.<sup>31</sup> As a negative control, we used the osteosarcoma U2OS cell line. As expected, zebrafish *tert*<sup>-/-</sup> tumors did not show telomerase activity (Figure 1K). Surprisingly, early *tert*<sup>+/+</sup> tumors also failed to show detectable telomerase activity. This result suggests that zebrafish melanoma does not activate telomerase at an early stage of tumorigenesis.

Cancer cells can also maintain telomeres by engaging in an alternative mechanism to telomerase known as ALT. ALT cells are characterized by an increase in the heterogeneity of telomere length, displaying longer and shorter telomeres than TERT-positive cells.<sup>32</sup> However, analyzing TRFs derived from both *tert*<sup>+/+</sup> and *tert*<sup>-/-</sup> tumors, we observed a similar spread of telomere sizes (Figures 1C and 1H). ALT is also characterized by the presence of extrachromosomal DNA, known as C-circles.<sup>33</sup> Amplification of telomeric circles using  $\Phi$ 29 DNA polymerase allows for the amplification of C-circles and provides a robust way to assess ALT-positive cells, such as U2OS.<sup>33</sup> However, this assay failed to detect the presence of C-circles in *tert*<sup>-/-</sup> tumors (Figures 1L and 1M).

Consistently, a previous study using Ras-induced zebrafish melanoma also did not exhibit an increase in C-circles.<sup>12</sup> Altogether, our data show that zebrafish melanoma initiation and early progression do not require telomerase and that these tumors do not engage in ALT to maintain telomere length.

### Lack of telomerase leads to growth restriction in late progression

Our observation that telomerase activation was not required for melanoma early progression prompted us to investigate its effect on later stages. We followed tumor progression over time and assessed the tumor area in fish aged 5, 7, and 9 months old (Figures 2A, 2B, and S3A). In 5-month-old fish, the average tumor area was indistinguishable between *tert*<sup>+/+</sup> and *tert*<sup>-/-</sup> fish. However, while *tert*<sup>+/+</sup> tumor size increased over time, the average area of *tert*<sup>-/-</sup> tumors remained stable and was significantly smaller than *tert*<sup>+/+</sup> tumors ( $p = 0.0269$  for 7 months;  $p = 0.0017$  for 9 months). Tumor size differences were more evident when individual tumor trajectories were taken into consideration (Figure 2C). All *tert*<sup>+/+</sup> tumors increased in size over time, while the size of most *tert*<sup>-/-</sup> tumors remained constant (Figure 2C). By calculating the regression slope for each tumor size variation (Figure 2D), we found that all *tert*<sup>+/+</sup> tumors had a positive trend, while most *tert*<sup>-/-</sup> tumors either did not grow (slope  $\approx 0$ ) or regressed. This result indicates that *tert*<sup>-/-</sup> tumors exhibited slower growth dynamics at later stages.

Although *tert*<sup>-/-</sup> tumors were smaller in size, they were as lethal as *tert*<sup>+/+</sup> tumors (Figure S3B). We previously reported that *tert*<sup>-/-</sup> fish age prematurely and exhibit reduced survival.<sup>26</sup> This effect could explain the high mortality of the *tert*<sup>-/-</sup> fish rather than the melanoma *per se*. To examine this reduced survival further, we analyzed the survival of cousins of the fish used in this study as a control (Figures S3B and S3C). The survival of fish lacking *mitfa:HRAS* was close to 100% throughout the experiment, and *tert*<sup>-/-</sup> did not differ from *tert*<sup>+/+</sup> fish. This suggests that the high mortality observed in *mitfa:HRAS*; *tert*<sup>-/-</sup> fish is not due to premature aging but rather is a consequence of the melanoma itself. Given the differences in tumor size, we also tested whether size could predict melanoma survival rates. To answer this question, we quantified the animals that survived until 9 months of age (“survivor” group) and the ones that died between 7 and 9 months (“deceased” group) for each given genotype (Figure 2E). We observed that tumor size did not differ between the survivor and deceased groups in *tert*<sup>+/+</sup> fish, indicating that tumor size did not predict survival for *tert*<sup>+/+</sup> animals (dashed and filled lines of *tert*<sup>+/+</sup> fish in Figure 2E). In contrast, the non-survival group of *tert*<sup>-/-</sup> fish possessed larger tumors than the survivor group ( $p = 0.0044$ ; dashed and filled lines of *tert*<sup>-/-</sup> fish in Figure 2E). This result indicates that tumor size greatly impacts the survival of *tert*<sup>-/-</sup> fish. It also shows that *tert*<sup>-/-</sup> tumors are capable of growing to the same extent as those of *tert*<sup>+/+</sup> fish (Figure 2E). However, in contrast to *tert*<sup>+/+</sup>, *tert*<sup>-/-</sup> fish carrying larger tumors die and are excluded from later stages of melanoma progression.

Our previous results showed that by 3 months of age, nearly all *tert*<sup>+/+</sup> and *tert*<sup>-/-</sup> fish possessed macroscopic tumors (Figure 2F) that were histologically comparable with similar invasiveness profiles (Figures 2G and 2H). In contrast, by 9 months of

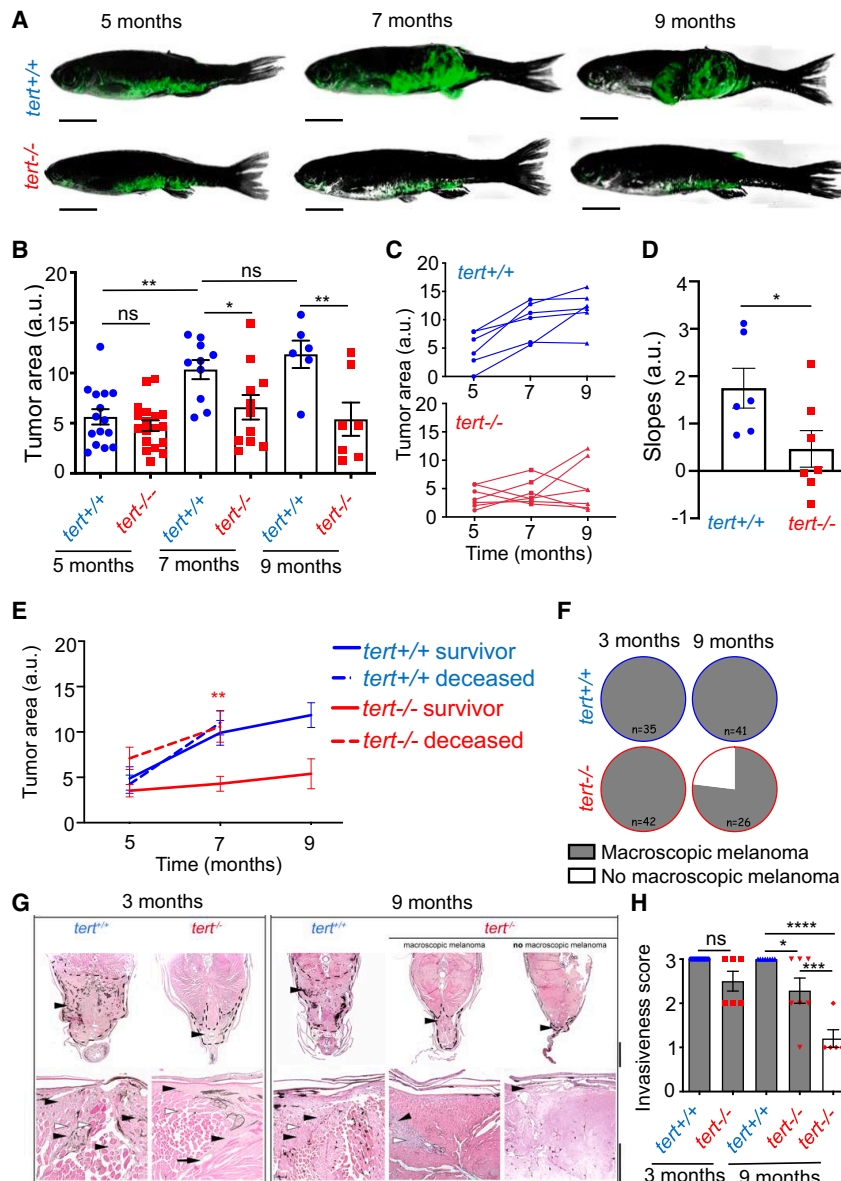


**Figure 2. Absence of telomerase restricts tumor growth, leading to melanoma regression**

(A–D) Lack of telomerase impacts late tumor growth. (A) Examples of melanoma evolution over time of *tert*<sup>+/+</sup> and *tert*<sup>-/-</sup> fish. Scale bars: 0.5 cm. (B) Quantification of tumor size of 5-, 7-, and 9-month-old *tert*<sup>+/+</sup> and *tert*<sup>-/-</sup> fish ( $n \geq 7$ ; one-way ANOVA). (C) Evolution tumor size over time in individual animals ( $n = 6$  and  $n = 7$ ). (D) Slope of tumor size evolution calculated using linear regression of three time points ( $n \geq 6$ ; unpaired t test). (E) Larger tumors are associated with *tert*<sup>-/-</sup> fish lethality. Tumor size evolution of fish that either survived until 9 months (solid line: survival group) or died after 7 months (dashed line: non-survivor group). Statistics compare *tert*<sup>-/-</sup> survivors with *tert*<sup>-/-</sup> deceased fish at 7 months ( $n \geq 7$ ; unpaired t test). (F–H) Melanoma regresses in fish lacking telomerase. (F) *tert*<sup>+/+</sup> and *tert*<sup>-/-</sup> fish with macroscopic tumors at 3 and 9 months of age. (G) Histopathology analysis of melanoma of 3- and 9-month-old *tert*<sup>+/+</sup> and *tert*<sup>-/-</sup> zebrafish. Tumors are indicated by a black arrowhead and dashed line. Higher magnification shows infiltrative features of melanoma (black arrowhead), with marked invasion, destruction, and replacement of the hypaxial muscle (white arrowhead). Top scale bar: 500  $\mu\text{m}$ , bottom scale bar: 200  $\mu\text{m}$ . (H) Quantification of melanoma invasiveness: (1) non-invasive, (2) minimally invasive, and (3) invasive ( $n \geq 5$ ; one-way ANOVA). Error bars represent  $\pm$  SEM; each dot represents an individual tumor; \* $p \leq 0.05$ , \*\* $p \leq 0.01$ , \*\*\* $p \leq 0.001$ , and \*\*\*\* $p \leq 0.0001$ . ns, not significant; a.u., arbitrary units.

age, while all *tert*<sup>+/+</sup> tumors still exhibited clear tumors, a significant proportion of *tert*<sup>-/-</sup> fish (~25%,  $n = 26$ ) lacked visible tumors, suggestive of melanoma regression (Figure 2F). We were still able to find histological remains of melanoma with reduced invasiveness in these fish (Figures 2G and 2H). Muscle fibers of regressing melanoma fish displayed signs of atrophy, with empty spaces between the fibers. A possible explanation could be that melanoma invaded the muscle, and when it regressed, the muscle fibers did not recover. The remaining macroscopic *tert*<sup>-/-</sup> tumors displayed significantly reduced invasiveness when compared to *tert*<sup>+/+</sup> tumors ( $p = 0.0257$ ; Figures 2G and 2H). Overall, our results suggest that *tert*<sup>-/-</sup> tumors can grow as much as *tert*<sup>+/+</sup> tumors, but they result in earlier mortality relative to *tert*<sup>+/+</sup> fish. Thus, not only is telomerase required to sustain tumor growth in late melanoma progression, but the lack of telomerase

increases the susceptibility of the organism to larger tumors. **Telomerase is re-activated in late melanoma progression** Given that late melanoma progression is defective upon telomerase deficiency, we sought to determine whether telomerase is re-activated in tumors of *tert*<sup>+/+</sup> fish. We assayed telomerase activity by TRAP in 9-month-old fish, and indeed, we were able to detect telomerase activity in *tert*<sup>+/+</sup> tumors but not, as expected, *tert*<sup>-/-</sup> tumors (Figure 3A). Thus, telomerase is re-activated in melanoma cells but only after tumors are formed and macroscopically visible. We next analyzed telomere length in tumors derived from 7-month-old fish using TRF (Figures 3B and 3C). We observed that while telomeres of *tert*<sup>-/-</sup> tumors are shorter than their matched skin controls, *tert*<sup>+/+</sup> tumors maintained an average telomere length similar to the skin (Figures 3B and 3C). Consistently, *tert*<sup>-/-</sup> tumors displayed greater levels of DNA damage foci at telomeres ( $p = 0.0421$ ; Figures 3D and 3E) than those observed in early-stage tumors (Figures 1E and 1F). It is striking that even in the absence of telomerase, *tert*<sup>-/-</sup> fish possessed tumors by 9 months of age. In order to verify whether these tumors

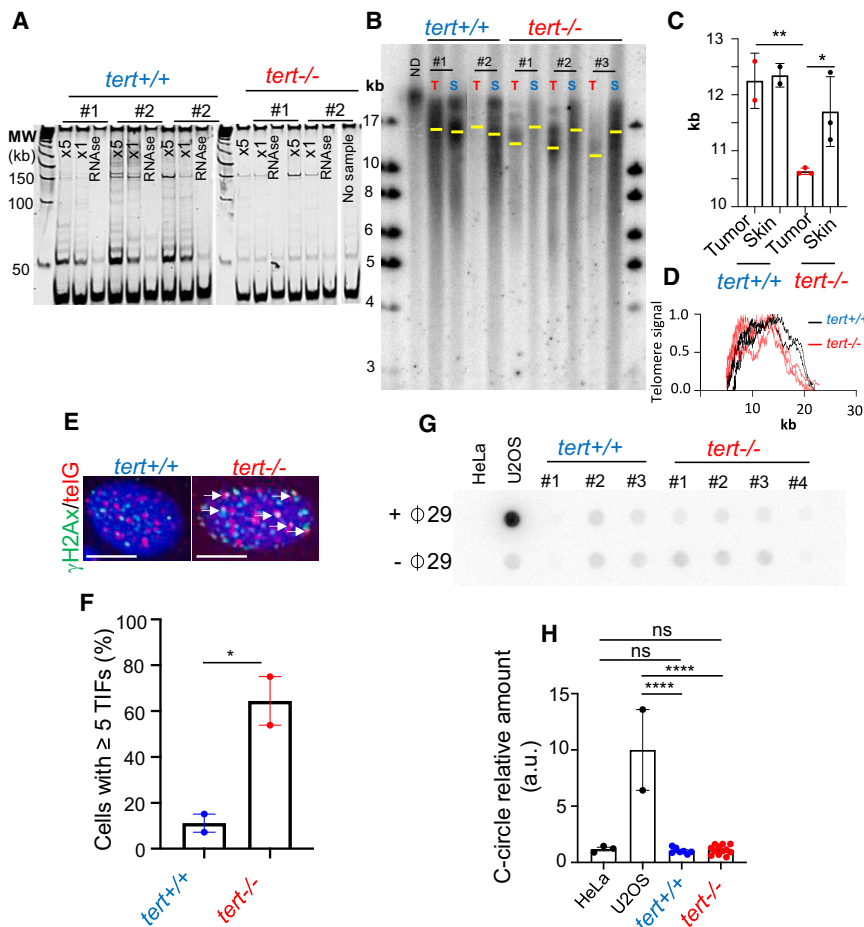


**Figure 3. Telomerase is re-activated in late-stage melanoma, and its absence causes telomere shortening**

(A–D) Telomerase is active in tumors of 9-month-old fish and telomere shortening occurs in *tert*<sup>-/-</sup> tumors. (A) Telomerase activity evaluated by TRAP in tumor samples derived from *tert*<sup>+/+</sup> and *tert*<sup>-/-</sup> 9-month-old fish ( $n = 3$  and  $n = 2$ , respectively). (B) Telomere restriction fragment (TRF) analysis by Southern blotting of tumor (T) and skin (S) genomic DNA extracted from 9-month-old fish (yellow bars represent mean telomere length) and (C) quantifications for mean telomere length and (D) densitometries of TRFs ( $n \geq 2$ ; one-way ANOVA).

(E) Images of  $\gamma$ H2Ax/telG immune-FISH of tumor cells derived from *tert*<sup>+/+</sup> and *tert*<sup>-/-</sup> 9-month-old fish. White arrows indicate telomere dysfunction-induction foci (TIFs) in tumor cells. Scale bars: 6  $\mu$ m.

(F) Percentage of cells containing  $\geq 5$  TIFs from (B) ( $n = 2$ ; unpaired t test).

(G and H) Late melanoma in *tert*<sup>-/-</sup> fish do not engage ALT as TMM. (G) C-circle assay of tumor samples derived from *tert*<sup>+/+</sup> and *tert*<sup>-/-</sup> 3-month-old fish. Extracts from HeLa cells and U2OS were used as negative and positive controls, respectively. (H) Quantification of C-circle signal ( $n \geq 7$ ; one-way ANOVA).

Error bars represent  $\pm$  SEM; each dot represents an individual tumor; \* $p \leq 0.05$ , \*\* $p \leq 0.01$ , and \*\*\*\* $p \leq 0.0001$ . ns, not significant.

developed ALT as a TMM, we looked for the presence of C-circles. Surprisingly, we did not obtain  $\Phi 29$  DNA polymerase amplification of C-circles in either *tert*<sup>+/+</sup> or *tert*<sup>-/-</sup> tumors (Figures 3F and 3G), denoting that *mitfa:HRAS* tumors do not activate ALT at later progression stages. Taking these results together, as expected from other models, telomerase is indeed expressed during melanoma progression in telomerase-proficient individuals. However, we highlight that telomerase activation is a late event in tumorigenesis and that it occurs upon telomere shortening and increased DNA damage at telomeres.

Interestingly, both late *tert*<sup>+/+</sup> and *tert*<sup>-/-</sup> tumors show a low mutational burden (Figure S4A) contrasting with human cutaneous melanoma, which characteristically exhibit a high number of mutations.<sup>34</sup> Our result is consistent with previous work showing a similar low mutation burden in *mitfa:BRAF*<sup>V600E</sup>; *tp53*<sup>-/-</sup> and *mitfa:NRAS*<sup>Q61K</sup> zebrafish melanoma models in the absence of UV light.<sup>34</sup> Surprisingly, the absence of telomerase did not change the mutational profile of melanoma, instead merely showing a global lower level of missense mutations in *tert*<sup>-/-</sup> tumors (Figure S4A). Moreover, we did not detect any mutational pattern between *tert*<sup>+/+</sup> and *tert*<sup>-/-</sup> tumors. Looking at specific genes that are important for telomere biology and/or melanoma formation, we found mostly synonymous mutations (Figure S4B), which are unlikely to affect protein function.

Examining the *tert* gene promoter, we found ETS-binding sites (GGAA/T), and an E-box (enhancer box), which were already present in the skin of WT fish, while no additional mutations were found in the tumors (Figure S4C). These results suggest that telomerase re-activation is not dependent on *de novo* ETS-binding sites in the *tert* gene promoter.

### Tumor-autonomous causes for *tert*<sup>-/-</sup> tumor growth decline

We showed that a lack of telomerase leads to telomere shortening and growth restriction in late melanoma progression. To understand the mechanism behind the restrained growth of *tert*<sup>-/-</sup> tumors, we compared the expression profiles of *tert*<sup>+/+</sup> versus *tert*<sup>-/-</sup> tumors with RNA sequencing (RNA-seq) using early-stage (3 months old; Figure S5A) and later-stage (9 months old; Figure 4A) melanoma tumor samples. Gene set enrichment analysis (GSEA) showed that proliferation pathways are downregulated in *tert*<sup>-/-</sup> tumors in 9-month-old fish, while apoptosis is upregulated (Figure 4B). We sought to confirm these results using immunofluorescence. We observed that DNA damage is increased in *tert*<sup>-/-</sup> melanoma at later stages ( $\gamma$ H2Ax,  $p = 0.0054$ ; Figure 4C). Consistently, we observed that cell proliferation rates are lower (proliferating cell nuclear antigen or PCNA,  $p < 0.0001$ ; Figure 4D) while apoptosis levels are higher (cleaved caspase-3,  $p = 0.005$ ; Figure 4E) in later-stage *tert*<sup>-/-</sup> melanoma. In contrast, we found no differences for these markers in tumors

GSEA hallmarks in *tert*<sup>-/-</sup> compared to *tert*<sup>+/+</sup>

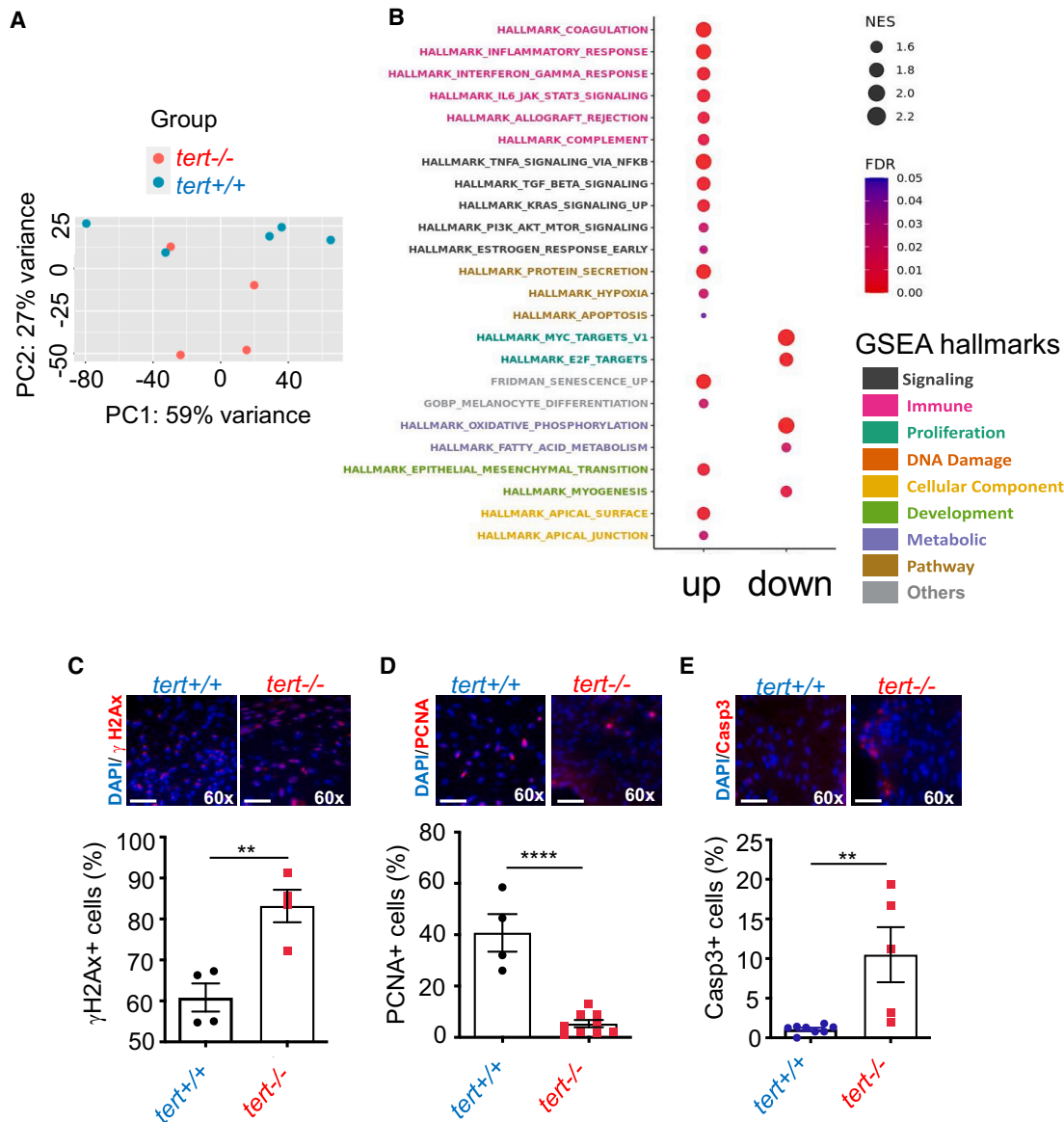


**Figure 4. Lack of telomerase leads to low proliferation and increased apoptosis, inflammation, and melanocyte differentiation**

(A) Principal-component analysis (PCA) based on untargeted transcriptomics data of tumors from 9-month-old fish.

(B) Gene set enrichment analysis (GSEA) hallmarks of late-stage melanoma of *tert*<sup>-/-</sup> fish compared to *tert*<sup>+/+</sup> highlighting inflammatory pathways, senescence, and melanocyte differentiation.

(C–E) Representative immunofluorescence images and respective quantifications of *tert*<sup>+/+</sup> and *tert*<sup>-/-</sup> tumors. Scale bars: 20 μm. (C) DNA damage by γH2AX, (D) proliferation by PCNA, and (E) apoptosis by cleaved caspase-3 immunofluorescence of 9-month-old fish tumors ( $n \geq 4$ ; unpaired t test).

Error bars represent  $\pm$  SEM; each dot represents an individual tumor;  $n \geq 4$ ; \* $p \leq 0.05$ , \*\* $p \leq 0.01$ , and \*\*\*\* $p \leq 0.0001$ .

derived from 3-month-old fish (Figures S5C–S5E). Nevertheless, GSEA showed incipient profiles of reduction in cell proliferation and higher apoptosis even in early *tert*<sup>-/-</sup> tumors (Figure S5B). Our results show that the lack of telomerase affects both cell cycle progression and cell survival. This finding could explain the differences in tumor growth between *tert*<sup>+/+</sup> and *tert*<sup>-/-</sup> fish at

a later stage of tumorigenesis. In addition, our expression profiles also show an increase in the expression of genes related to melanocyte differentiation, suggesting that melanoma cells may exhibit a propensity to differentiate back to melanocytes. Consistently, melanocyte differentiation of melanoma cells was previously identified as one of the major expression signatures

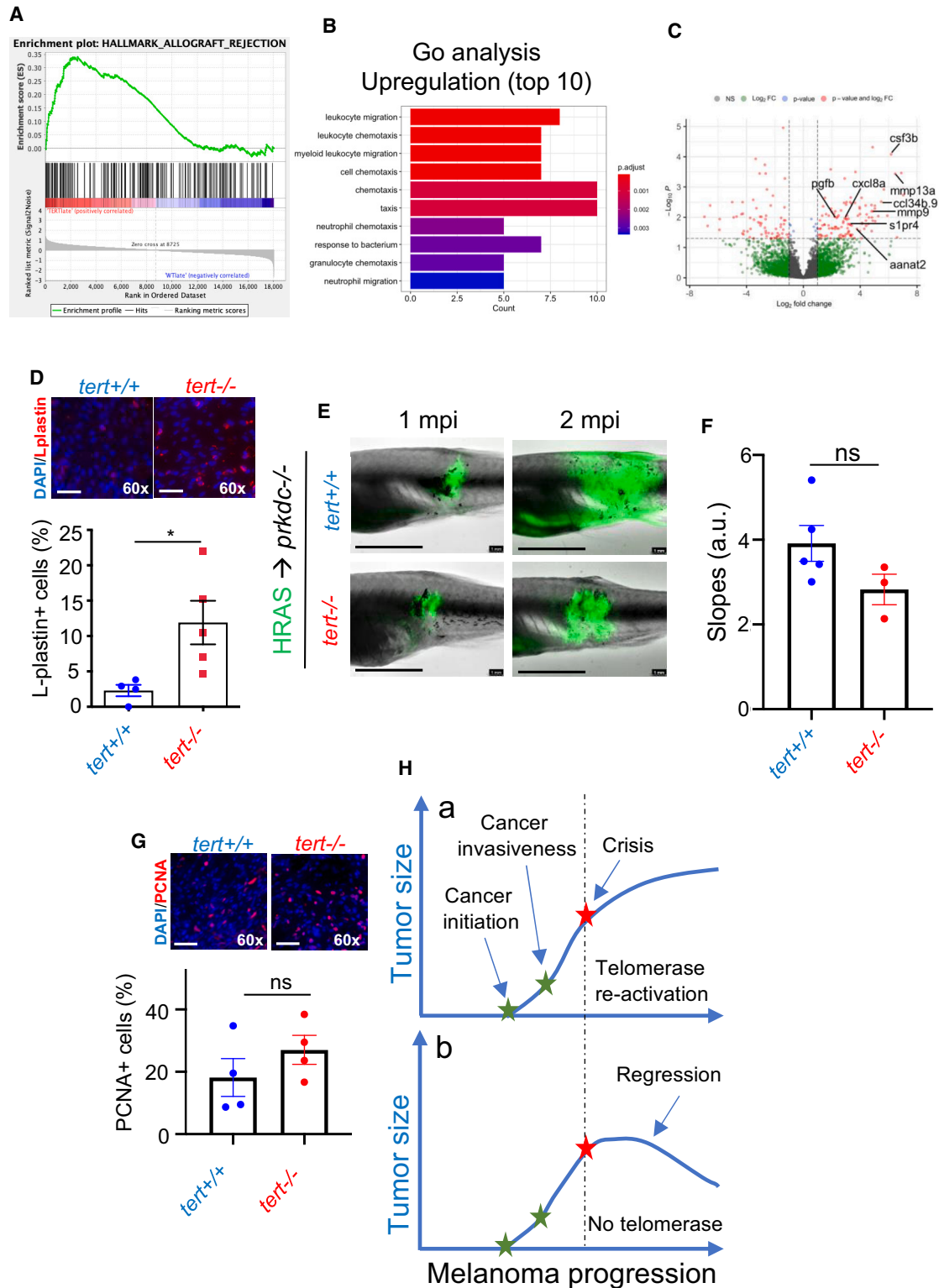


**Figure 5. The immune system restrains growth of telomerase-deficient melanoma**

Telomerase-deficient tumors are strongly immunogenic.

(A) Allograft rejection enrichment plot.

(B) Gene Ontology (GO) enrichment analysis for upregulated genes of late-stage melanoma of *tert*<sup>-/-</sup> fish compared to *tert*<sup>+/+</sup>.

(legend continued on next page)

of regressing melanomas in the unique melanoma-bearing Libe-  
chov (MeLiM) minipig model.<sup>35</sup> Our data indicate that growth re-  
striction of late *tert*<sup>-/-</sup> melanoma encompasses a tumor-auton-  
omous effect by reducing cell proliferation and increasing  
apoptosis and melanocyte differentiation. Interestingly, similar  
GSEA patterns were observed in a previous study focused on  
the non-canonical functions of mouse telomerase, including  
E2F targets, oxidative phosphorylation, and mTOR pathways.  
This suggests that the non-canonical roles of telomerase are  
likely involved in our model as well.<sup>36</sup>

### Non-tumor-autonomous causes for *tert*<sup>-/-</sup> tumor growth decline

GSEA also revealed that upregulation of the immune system was  
a hallmark of late *tert*<sup>-/-</sup> melanomas (Figure 4B). Interestingly,  
one of the inflammation GSEA pathways upregulated in late  
*tert*<sup>-/-</sup> was allograft rejection (Figures 4B and 5A). Gene expres-  
sion profiles consistent with immune system alterations were  
already present in early *tert*<sup>-/-</sup> tumors, despite ranking among  
the fourth-most significant cellular networks affected at that  
time point (Figure S5B). Also, Gene Ontology (GO) enrichment  
analyses for the tumors in the 9-month-old fish (Figures 5B and  
5C) reinforce the idea that the immune system might play an  
important role in late *tert*<sup>-/-</sup> melanomas. In order to test whether  
*tert*<sup>-/-</sup> tumors were more immunogenic, we compared levels of  
immune infiltrates in melanoma of early and late tumors. We per-  
formed immunofluorescence staining for immune cells, and this  
analysis revealed a robust tumor infiltration of the late-stage  
*tert*<sup>-/-</sup> tumors (L-plastin,  $p = 0.0310$ ; Figure 5D), although  
some infiltration could be detected in early *tert*<sup>-/-</sup> tumors ( $p =$   
 $0.0493$ ; Figure S5F). Our results show that *tert*<sup>-/-</sup> melanoma is  
more immunogenic than *tert*<sup>+/+</sup> tumors. Our data also suggest  
that an immune response may play a role in restricting the later  
stages of growth of *tert*<sup>-/-</sup> melanomas. In agreement, regressing  
melanoma of MeLiM minipigs was also shown to be accompa-  
nied by a robust immune response.<sup>35</sup>

To test the idea that the immune system could restrain the  
growth of *tert*<sup>-/-</sup> melanomas, we transplanted melanoma cells  
derived from 9-month-old tumors into immunocompromised pro-  
tein kinase DNA-activated catalytic subunit (*prkdc*<sup>-/-</sup>) mutant  
fish. These fish are deficient in DNAPk and lack mature B and  
T cells.<sup>37</sup> We assessed tumor growth between 1 and 2 months af-  
ter transplantation. Consistent with previous data, *tert*<sup>+/+</sup> tumors  
increased in size over this period (Figure 5E). Strikingly, despite  
a more restrained growth, *tert*<sup>-/-</sup> tumors also increased in size  
when transplanted into immunocompromised fish ( $p = 0.1312$ ;  
Figures 5E and 5F). To show that the increase in tumor size was

due to cell division rather than simple cell expansion, we  
measured cell proliferation by immunofluorescence. Indeed, the  
rates of cell proliferation were similar between *tert*<sup>+/+</sup> and *tert*<sup>-/-</sup>  
tumors ( $p = 0.2872$ ; Figure 5G), denoting that *tert*<sup>-/-</sup> tumor cells  
were capable of sustained cell proliferation. Unfortunately, due  
to high mortality, we were unable to observe tumor growth  
beyond 2 months post-injection. Finally, to test whether the trans-  
planted *tert*<sup>-/-</sup> tumors were a selection of cells that activated a  
TMM, we measured C-circles to assess ALT activation. Similar  
to the original tumors in *tert*<sup>-/-</sup> fish, we did not detect any signs  
of ALT in the transplanted tumors ( $p > 0.9999$  compared to  
HeLa; Figures S6A and S6B). Altogether, our results indicate  
that even though *tert*<sup>-/-</sup> tumors stagnate and even regress in  
*tert*<sup>-/-</sup> fish, when transplanted to an immunocompromised envi-  
ronment, they can proliferate and grow in size. Thus, not only are  
*tert*<sup>-/-</sup> tumors more immunogenic, but they are also restrained  
from growth by the organism adaptive immune system, similar  
to what has been observed in humans through CD8-positive cyto-  
toxic T lymphocytes.<sup>35,38</sup>

## DISCUSSION

The identification of activating TPMs in a high frequency for  
several human cancers, including cutaneous melanoma,<sup>20,21,24</sup>  
highlights the role of telomere protection and TMMs in tumori-  
genesis. Previous studies provided evidence that TPMs may  
occur as an early step in carcinogenesis. This event would likely  
confer an advantageous evolutionary step rendering cell immor-  
tality to early cancer precursors. However, the absolute require-  
ment of a TMM for early tumorigenesis is still unclear.

In our current study, the absence of telomerase in two estab-  
lished zebrafish melanoma models (HRAS and BRAF) results in  
the same tumor incidence as WT controls. Additionally, early  
*tert*<sup>-/-</sup> tumors display similar invasiveness levels and tumor  
size to *tert*<sup>+/+</sup>. Thus, contrary to our initial expectation, telome-  
rase is not required for melanoma initiation and early progression  
in zebrafish. These results are also surprising when taking into  
consideration that late-generation telomerase-deficient mice  
(G5 *Terc*<sup>-/-</sup>) are resistant to skin tumorigenesis.<sup>11</sup> A potential dif-  
ference between these models may reside in the fact that G5  
*Terc*<sup>-/-</sup> mice have considerably shorter telomeres from birth.<sup>11</sup>  
Thus, G5 *Terc*<sup>-/-</sup> pre-cancer cells would attempt to proliferate  
with short telomeres capable of restricting cell proliferation. In  
contrast, *tert*<sup>-/-</sup> zebrafish possesses normal telomere length  
during development, and differences are only visible in adult  
fish, as they result from *tert*<sup>+/-</sup> intercrosses. Indeed, we fail to  
detect telomere shorting in early melanoma of either *tert*<sup>+/+</sup> or

(C) Volcano plot of differentially expressed genes of late-stage melanoma of *tert*<sup>-/-</sup> fish compared to *tert*<sup>+/+</sup>, highlighting genes included in leukocyte migration pathway from the GO analysis.

(D) Immunofluorescence images and quantifications of immune cell infiltrates (L-plastin) of late-stage melanoma. Late-stage *tert*<sup>-/-</sup> melanoma is able to proliferate and grow in immunocompromised fish ( $n \geq 4$ ; unpaired t test). Scale bars: 20  $\mu\text{m}$ .

(E) Images of immunocompromised zebrafish (*prkdc*<sup>-/-</sup>) engrafted with primary melanoma cells derived from 9-month-old zebrafish at 1 and 2 months post-injection (mpi). Scale bars: 0.5 cm.

(F) Progression slope of tumor area calculated by a linear regression of two time points (1 and 2 mpi) ( $n \geq 4$ ; unpaired t test).

(G) Cell proliferation of tumor cells quantified using PCNA immunofluorescence ( $n \geq 4$ ; unpaired t test). Scale bars: 20  $\mu\text{m}$ .

(H) We propose that melanoma can initiate and progress without telomerase activation. However, once telomeres become critically short, cancer cells must activate telomerase to sustain proliferation at later stages (a). If they fail to do so, tumor growth stagnates, leading to tumor regression (b).

Error bars represent  $\pm$  SEM; each dot represents an individual tumor; \* $p \leq 0.05$ . ns, not significant.

*tert*<sup>-/-</sup> fish. This may occur because melanomas, at this stage, have not yet undergone enough cell divisions to show an appreciable reduction of average telomere length when compared to skin controls. Alternatively, melanoma initiation in the *mitfa:HRAS* model may not have a single origin, leading to multiple clones with different telomere lengths.

Similar to early *tert*<sup>-/-</sup> melanoma, we observe neither telomerase activity nor appreciable telomere shortening in *tert*<sup>+/+</sup> tumors. However, in early *tert*<sup>-/-</sup> tumors, we already observe a small increase in DNA damage at telomeres, which could suggest that at least a minority of *tert*<sup>+/+</sup> melanoma cells activate telomerase at an early stage but below the detectable level. This finding is consistent with the similar tumor incidence observed in *tert*<sup>+/+</sup> or *tert*<sup>-/-</sup> fish, arguing that critical telomere shortening fails to restrain tumorigenesis at early stages of melanoma formation. This result differs from previous observations that link TPMs to an early event in tumorigenesis.<sup>30</sup> However, Chiba et al. demonstrated that, despite carrying TPMs, human melanoma cells still shorten telomere length with similar kinetics to other primary cells and that telomerase upregulation only occurs after many cell divisions, concomitant with an accumulation of critically short telomeres.<sup>30</sup> Thus, even though TPMs may occur early in tumorigenesis, telomere length in pre-cancer cells may be sufficient to sustain early cell divisions so that the activation of telomerase and telomere elongation constitute a later event required to sustain continuous tumor growth. Consistent with this notion, Viceconte et al. identified a set of aggressive human melanoma metastases that did not present either telomerase activity or ALT as TMMs.<sup>15</sup> Our work appears to replicate these findings of human melanoma and, thus, constitute a timely animal model to study cancers that fail to activate a TMM.

In contrast to early melanoma, we observed that telomerase becomes active at later stages, while its absence restricts tumor growth, leading to tumor regression. These results reaffirm the requirement of a TMM in tumorigenesis, albeit at an unsuspected later stage of cancer progression. Nevertheless, melanoma results in zebrafish mortality, even in the absence of TMMs. Interestingly, tumor size in *tert*<sup>+/+</sup> fish did not correlate with mortality, whereas larger tumors in *tert*<sup>-/-</sup> fish were more likely to be fatal. Although we show that *tert*<sup>-/-</sup> fish did not die more frequently due to premature aging alone (a feature of the *tert*<sup>-/-</sup> mutants), we believe that the combination of *tert* tumors that continue to grow and the inherent fragility of *tert* fish is responsible for the increased mortality. Ackermann et al. reported that half of studied neuroblastomas, a pediatric tumor of the sympathetic nervous system, also did not possess a TMM.<sup>39</sup> Neuroblastomas lacking TMMs were also associated with spontaneous regression followed by better prognosis.

Cases of human melanoma regression also occur at often unsuspected rates, accounting for 10%–35% of the totality of melanomas.<sup>40</sup> However, the mechanism of human melanoma regression is currently unknown. We propose that telomere shortening may account for melanoma regression by imposing a 2-fold barrier to tumor growth: (1) a “classical” tumor-autonomous mechanism whereby short telomeres restrain cell division while inducing apoptosis and melanocyte differentiation. Consistently, melanoma regression in other models is also accompanied by cell-cycle arrest, apoptosis, and melanocyte

differentiation,<sup>35,41</sup> even though telomere shortening was not assessed as a potential cause. (2) A second unsuspected barrier consisting of a non-tumor-autonomous mechanism imposed by the immune system. *tert*<sup>-/-</sup> tumors are more immunogenic, possessing higher numbers of immune cell infiltrates. Consistently, GSEA of *tert*<sup>-/-</sup> tumors highlighted the upregulation of immune response pathways, including terms such as allograft rejection. Conclusively, *tert*<sup>-/-</sup> tumors were able to proliferate and grow once transplanted into immunocompromised fish lacking B and T cells. This second barrier was previously observed in regressing melanoma of MeLiM minipigs and humans, in particular through CD8-positive cytotoxic T lymphocytes.<sup>35,38</sup> In agreement with our data, human cancers harboring mutations in TERT were previously highlighted as immunogenic, leading to better survival upon immunotherapy.<sup>18,19</sup> In addition, melanoma susceptible to immune checkpoint therapy had less expression of genes related to telomere maintenance.<sup>17</sup> Conversely, TPMs leading to telomerase expression were associated with resistance to immunotherapy in metastatic renal cell carcinoma, being proposed as a negative predictor of outcome for immunotherapy.<sup>42</sup> Altogether, these studies suggest that telomerase expression protects tumors from being a target of the immune system.

In summary, our data show that telomerase is not required for the initiation and early progression of melanoma in zebrafish (Figure 5Ha). However, once telomeres reach a critical threshold of erosion, cells re-activate telomerase to sustain cell proliferation and cancer growth. If they fail to do so, telomeres continue to shorten (Figure 5Hb), and tumors stagnate growth and even regress. This is caused by two mechanisms: a tumor-autonomous mechanism (cell-cycle arrest, apoptosis, and melanocyte differentiation) and a non-tumor-autonomous mechanism (immune response). Our results illuminate an unappreciated contribution of the immune system in tumor formation in telomerase-negative tumors. We found that, despite the apparent lack of dependency on a TMM in tumor initiation and early progression, later stages of melanoma growth are influenced by immune function. It remains to be tested if immune activation in human tumors with critically eroded telomeres may enhance the ability to impair tumor growth.

### Limitations of the study

To investigate whether *tert*<sup>-/-</sup> tumor cells were immortal, we attempted to grow transplanted cells *in vitro*. However, this was unsuccessful due to suboptimal protocols and the need for specialized media for zebrafish cell cultures. Simultaneously, we tried to perform multiple rounds of tumor transplantations but could not recover sufficient melanoma cells from the host fish, as the tumors had spread extensively throughout the host tissue.

We also attempted to induce melanoma regression by treating *mitfa:HRAS*, *tert*<sup>+/+</sup> fish with telomerase drug inhibitors but failed to see regression with the doses and treatment durations tested.

Lastly, from these findings alone, it is not known how telomere shortening triggers an immune response observed in late tumors. The profile of the immune response observed in this study is also not fully understood. Telomerase-deficient tumors may become increasingly immunogenic. Alternatively, an immune system with short telomeres may become more reactive.

## RESOURCE AVAILABILITY

### Lead contact

Further information and requests for resources should be directed to and will be fulfilled by the lead contact, Miguel Godinho Ferreira ([miguel-godinho.ferreira@unice.fr](mailto:miguel-godinho.ferreira@unice.fr)).

### Materials availability

This study did not generate new unique reagents.

### Data and code availability

- Raw RNA-seq and DNA sequencing data have been deposited at the NCBI and ENA databases, respectively, and are publicly available as of the date of publication. Accession numbers are listed in the [key resources table](#).
- The code that we developed to analyze our RNA-seq data is publicly available as of the date of publication. The link to the code is listed in the [key resources table](#).
- Any additional information required to reanalyze the data reported in this paper is available from the [lead contact](#) upon request.

## ACKNOWLEDGMENTS

We are grateful to Lea Harrington (University of Toronto, Canada) and Elizabeth Patton (University of Edinburgh, UK) for critically reading our manuscript. We also thank Richard White (University of Oxford) for kindly providing the ZMEL cell line. This work was supported by the Portuguese Fundação para a Ciência e a Tecnologia (FCT; PTDC/BIM-ONC/3402/2014), Université Côte d'Azur - Académie 4 (Installation Grant: Action 2-2019), Fondation ARC pour la Recherche sur le Cancer (PJA20161205137), Institut National Du Cancer (INCa; PLBIO21-228), and the Howard Hughes Medical Institute International Early Career Scientist grant awarded to M.G.F. B.L.-B. was supported by a postdoctoral fellowship awarded by the Fondation pour la Recherche Médicale (FRM; SPF201809007006). We thank the Instituto Gulbenkian de Ciência (IGC) Histology Unit, the IGC Imaging Unit, and the IGC Fish Facility for excellent animal care and assistance with experimental planning and sample and data collection. The IGC Fish Facility is financed by Congento LISBOA-01-0145-FEDER-022170, co-financed by FCT (Portugal) and Lisboa2020, under the PORTUGAL2020 agreement (European Regional Development Fund). The work was also performed in the PEMA Fish Facility, Imaging Core Facility (PICMI), and the Genomics facilities at the IRCAN supported by FEDER, Région Provence-Alpes-Côte d'Azur, Conseil Départemental 06, ITMO Cancer Aviesan (plan cancer), Cancéropole Provence Alpes-Côte d'Azur, Gis Ibsa, CNRS, and INSERM. The funders had no role in study design, data collection and analysis, decision to publish, or preparation of the manuscript.

## AUTHOR CONTRIBUTIONS

B.L.-B. performed the experiments and carried out data analyses; J.N. and T.F. performed the BRAF experiments; T.F. and M.E.M. performed and analyzed TRFs; S.T. quantified IFs; J.-X.Y., D.K., and M.B. performed transcriptomics analyses; T.G.C. performed histopathology analyses; G.A. performed the maternal *tert* mRNA contribution experiment; L.T. and G.L. analyzed the DNA sequencing data; B.L.-B. and M.G.F. conceived the study, designed the experiments, and wrote the manuscript; and M.G.F. supervised the work.

## DECLARATION OF INTERESTS

The authors declare no competing interests.

## STAR★METHODS

Detailed methods are provided in the online version of this paper and include the following:

- [KEY RESOURCES TABLE](#)
- [EXPERIMENTAL MODEL AND STUDY PARTICIPANT DETAILS](#)

- Ethics statement
- Zebrafish maintenance
- Cell culture
- [METHOD DETAILS](#)
  - Fixation for histology and immunofluorescence
  - Immunofluorescence of paraffin embedded zebrafish
  - Sample collection
  - Telomere restriction fragment (TRF) analysis by Southern blot
  - C-circle assay
  - TRAP assay
  - RNA extraction/RNA sequencing
  - Tumor allografts
  - Telomere dysfunction-induced focus (TIF)
- [QUANTIFICATION AND STATISTICAL ANALYSIS](#)
  - Tumor size quantification
  - Statistical analysis
- [ADDITIONAL RESOURCES](#)

## SUPPLEMENTAL INFORMATION

Supplemental information can be found online at <https://doi.org/10.1016/j.celrep.2024.115035>.

Received: April 22, 2024

Revised: October 29, 2024

Accepted: November 14, 2024

## REFERENCES

1. Aubert, G., and Lansdorp, P.M. (2008). Telomeres and aging. *Physiol. Rev.* *88*, 557–579.
2. Harley, C.B., Futcher, A.B., and Greider, C.W. (1990). Telomeres shorten during ageing of human fibroblasts. *Nature* *345*, 458–460.
3. Verdun, R.E., and Karlseder, J. (2007). Replication and protection of telomeres. *Nature* *447*, 924–931.
4. Maciejowski, J., and De Lange, T. (2017). Telomeres in cancer: Tumour suppression and genome instability. *Nat. Rev. Mol. Cell Biol.* *18*, 175–186.
5. Wright, W.E., Pereira-Smith, O.M., and Shay, J.W. (1989). Reversible cellular senescence: implications for immortalization of normal human diploid fibroblasts. *Mol. Cell Biol.* *9*, 3088–3092.
6. Shay, J.W., and Wright, W.E. (2011). Role of telomeres and telomerase in cancer. *Semin. Cancer Biol.* *21*, 349–353.
7. Kim, N.W., Piatyszek, M.A., Prowse, K.R., Harley, C.B., West, M.D., Ho, P.L.C., Coviello, G.M., Wright, W.E., Weinrich, S.L., and Shay, J.W. (1994). Specific Association of Human Telomerase Activity with Immortal Cells and Cancer. *Science* *266*, 2011–2015.
8. Blackburn, E.H., and Collins, K. (2011). Telomerase: An RNP enzyme synthesizes DNA. *Cold Spring Harb. Perspect. Biol.* *3*, a003558–a003559.
9. Pickett, H.A., and Reddel, R.R. (2015). Molecular mechanisms of activity and derepression of alternative lengthening of telomeres. *Nat. Struct. Mol. Biol.* *22*, 875–880.
10. Hu, J., Hwang, S.S., Liesa, M., Gan, B., Sahin, E., Jaskelioff, M., Ding, Z., Ying, H., Boutin, A.T., Zhang, H., et al. (2012). Antitelomerase therapy provokes ALT and mitochondrial adaptive mechanisms in cancer. *Cell* *148*, 651–663.
11. González-Suárez, E., Samper, E., Flores, J.M., and Blasco, M.A. (2000). Telomerase-deficient mice with short telomeres are resistant to skin tumorigenesis. *Nat. Genet.* *26*, 114–117.
12. Idilli, A.I., Cusanelli, E., Pagani, F., Berardinelli, F., Bernabé, M., Cayuela, M.L., Poliani, P.L., and Mione, M.C. (2020). Expression of *tert* Prevents ALT in Zebrafish Brain Tumors. *Front. Cell Dev. Biol.* *8*, 1–18.
13. Barthel, F.P., Wei, W., Tang, M., Martinez-Ledesma, E., Hu, X., Amin, S.B., Akdemir, K.C., Seth, S., Song, X., Wang, Q., et al. (2017). Systematic

- analysis of telomere length and somatic alterations in 31 cancer types. *Nat. Genet.* **49**, 349–357.
14. Dagg, R.A., Pickett, H.A., Neumann, A.A., Napier, C.E., Henson, J.D., Teber, E.T., Arthur, J.W., Reynolds, C.P., Murray, J., Haber, M., et al. (2017). Extensive Proliferation of Human Cancer Cells with Ever-Shorter Telomeres. *Cell Rep.* **19**, 2544–2556.
  15. Viceconte, N., Dheur, M.S., Majerova, E., Pierreux, C.E., Baurain, J.F., van Baren, N., and Decottignies, A. (2017). Highly Aggressive Metastatic Melanoma Cells Unable to Maintain Telomere Length. *Cell Rep.* **19**, 2529–2543.
  16. Ackermann, S., Cartolano, M., Hero, B., Welte, A., Kahlert, Y., Roderwieser, A., Bartenhagen, C., Walter, E., Gecht, J., Kerschke, L., et al. (2018). A mechanistic classification of clinical phenotypes in neuroblastoma. *Science* **362**, 1165–1170.
  17. Zhang, G., Wu, L.W., Mender, I., Barzily-Rokni, M., Hammond, M.R., Ope, O., Cheng, C., Vasilopoulos, T., Randell, S., Sadek, N., et al. (2018). Induction of Telomere Dysfunction Prolongs Disease Control of Therapy-Resistant Melanoma. *Physiol. Behav.* **24**, 4771–4784.
  18. Jiang, T., Jia, Q., Fang, W., Ren, S., Chen, X., Su, C., Zhang, L., and Zhou, C. (2020). Pan-cancer analysis identifies TERT alterations as predictive biomarkers for immune checkpoint inhibitors treatment. *Clin. Transl. Med.* **10**, e109.
  19. Li, H., Li, J., Zhang, C., Zhang, C., and Wang, H. (2020). TERT mutations correlate with higher TMB value and unique tumor microenvironment and may be a potential biomarker for anti-CTLA4 treatment. *Cancer Med.* **9**, 7151–7160.
  20. Horn, S., Figl, A., Rachakonda, P.S., Fischer, C., Sucker, A., Gast, A., Kadel, S., Moll, I., Nagore, E., Hemminki, K., et al. (2013). TERT promoter mutations in familial and sporadic melanoma. *Science* **339**, 959–961.
  21. Huang, F.W., Hodis, E., Xu, M.J., Kryukov, G.V., Chin, L., and Garraway, L.A. (2013). Highly recurrent TERT promoter mutations in human melanoma. *Science* **339**, 957–959.
  22. Jafri, M.A., Ansari, S.A., Alqahtani, M.H., and Shay, J.W. (2016). Roles of telomeres and telomerase in cancer, and advances in telomerase-targeted therapies. *Genome Med.* **8**, 69.
  23. Killela, P.J., Reitman, Z.J., Jiao, Y., Bettgowda, C., Agrawal, N., Diaz, L.A., Jr., Friedman, A.H., Friedman, H., Gallia, G.L., Giovannella, B.C., et al. (2013). TERT promoter mutations occur frequently in gliomas and a subset of tumors derived from cells with low rates of self-renewal. *Proc. Natl. Acad. Sci. USA* **110**, 6021–6026.
  24. Akbani, R., Akdemir, K., Aksoy, B., Albert, M., Ally, A., Amin, S., Arachchi, H., Arora, A., Auman, J., Ayala, B., et al. (2015). Genomic Classification of Cutaneous Melanoma. *Cell* **161**, 1681–1696.
  25. Shain, A.H., Yeh, I., Kovalyshyn, I., Sriharan, A., Talevich, E., Gagnon, A., Dummer, R., North, J., Pincus, L., Ruben, B., et al. (2015). The Genetic Evolution of Melanoma from Precursor Lesions. *N. Engl. J. Med.* **373**, 1926–1936.
  26. Henriques, C.M., Carneiro, M.C., Tenente, I.M., Jacinto, A., and Ferreira, M.G. (2013). Telomerase Is Required for Zebrafish Lifespan. *PLoS Genet.* **9**, e1003214.
  27. Michailidou, C., Jones, M., Walker, P., Kamarashev, J., Kelly, A., and Hurlstone, A.F.L. (2009). Dissecting the roles of Raf- and PI3K-signalling pathways in melanoma formation and progression in a zebrafish model. *Dis. Model. Mech.* **2**, 399–411.
  28. Patton, E.E., Widlund, H.R., Kutok, J.L., Kopani, K.R., Amatruda, J.F., Murphy, R.D., Berghmans, S., Mayhall, E.A., Traver, D., Fletcher, C.D.M., et al. (2005). BRAF Mutations Are Sufficient to Promote Nevi Formation and Cooperate with p53 in the Genesis of Melanoma. *Curr. Biol.* **15**, 249–254.
  29. Chin, L., Artandi, S.E., Shen, Q., Tam, A., Lee, S.L., Gottlieb, G.J., Greider, C.W., and DePinho, R.A. (1999). P53 Deficiency Rescues the Adverse Effects of Telomere Loss and Cooperates With Telomere Dysfunction To Accelerate Carcinogenesis. *Cell* **97**, 527–538.
  30. Chiba, K., Lorbeer, F.K., Shain, A.H., McSwiggen, D.T., Schruf, E., Oh, A., Ryu, J., Darzacq, X., Bastian, B.C., and Hockemeyer, D. (2017). Mutations in the promoter of the telomerase gene TERT contribute to tumorigenesis by a two-step mechanism. *Science* **357**, 1416–1420.
  31. Heilmann, S., Ratnakumar, K., Langdon, E., Kansler, E., Kim, I., Campbell, N.R., Perry, E., McMahon, A., Kaufman, C., van Rooijen, E., et al. (2016). A quantitative system for studying metastasis using transparent zebrafish. *Cancer Res.* **75**, 4272–4282.
  32. Henson, J.D., Neumann, A.A., Yeager, T.R., and Reddel, R.R. (2002). Alternative lengthening of telomeres in mammalian cells. *Oncogene* **21**, 598–610.
  33. Henson, J.D., Cao, Y., Huschtscha, L.I., Chang, A.C., Au, A.Y.M., Pickett, H.A., and Reddel, R.R. (2009). DNA C-circles are specific and quantifiable markers of alternative-lengthening-of-telomeres activity. *Nat. Biotechnol.* **27**, 1181–1185.
  34. Yen, J., White, R.M., Wedge, D.C., Van Loo, P., de Ridder, J., Capper, A., Richardson, J., Jones, D., Raine, K., Watson, I.R., et al. (2013). The genetic heterogeneity and mutational burden of engineered melanomas in zebrafish models. *Genome Biol.* **14**, R113.
  35. Rambow, F., Piton, G., Bouet, S., Leplat, J.J., Baulande, S., Marrau, A., Stam, M., Horak, V., and Vincent-Naulleau, S. (2008). Gene expression signature for spontaneous cancer regression in melanoma pigs. *Neoplasia* **10**, 714–726.
  36. Hasegawa, K., Zhao, Y., Garbuzov, A., Corces, M.R., Neuhöfer, P., Gillespie, V.M., Cheung, P., Belk, J.A., Huang, Y.H., Wei, Y., et al. (2024). Clonal inactivation of TERT impairs stem cell competition. *Nature* **632**, 201–208.
  37. Moore, J.C., Tang, Q., Yordán, N.T., Moore, F.E., Garcia, E.G., Lobbardi, R., Ramakrishnan, A., Marvin, D.L., Anselmo, A., Sadreyev, R.I., and Langenau, D.M. (2016). Single-cell imaging of normal and malignant cell engraftment into optically clear prkdc-null scid zebrafish. *J. Exp. Med.* **213**, 2575–2589.
  38. Aung, P.P., Nagarajan, P., and Prieto, V.G. (2017). Regression in primary cutaneous melanoma: etiopathogenesis and clinical significance. *Lab. Invest.* **97**, 657–668.
  39. Ackermann, S., Cartolano, M., Hero, B., Welte, A., Kahlert, Y., Roderwieser, A., Bartenhagen, C., Walter, E., Gecht, J., Kerschke, L., et al. (2018). A mechanistic classification of clinical phenotypes in neuroblastoma. *Science* **362**, 1165–1170.
  40. BLESSING, K., and McLAREN, K.M. (1992). Histological regression in primary cutaneous melanoma: recognition, prevalence and significance. *Histopathology* **20**, 315–322.
  41. Lister, J.A., Capper, A., Zeng, Z., Mathers, M.E., Richardson, J., Paranthaman, K., Jackson, I.J., and Elizabeth Patton, E. (2014). A conditional zebrafish MITF mutation reveals MITF levels are critical for melanoma promotion vs. regression in vivo. *J. Invest. Dermatol.* **134**, 133–140.
  42. Dizman, N., Lyou, Y., Salgia, N., Bergerot, P.G., Hsu, J., Enriquez, D., Izatt, T., Trent, J.M., Byron, S., and Pal, S. (2020). Correlates of clinical benefit from immunotherapy and targeted therapy in metastatic renal cell carcinoma: Comprehensive genomic and transcriptomic analysis. *J. Immunother. Cancer* **8**, e000953.
  43. Scahill, C.M., Digby, Z., Sealy, I.M., White, R.J., Wali, N., Collins, J.E., Stemple, D.L., and Busch-Nentwich, E.M. (2017). The age of heterozygous telomerase mutant parents influences the adult phenotype of their offspring irrespective of genotype in zebrafish. *Wellcome Open Res.* **2**, 77.
  44. Henson, J.D., Lau, L.M., Koch, S., Martin La Rotta, N., Dagg, R.A., and Reddel, R.R. (2017). The C-Circle Assay for alternative-lengthening-of-telomeres activity. *Methods* **114**, 74–84.
  45. Liberzon, A., Subramanian, A., Pinchback, R., Thorvaldsdóttir, H., Tamayo, P., and Mesirov, J.P. (2011). Molecular signatures database (MSigDB) 3.0. *Bioinformatics* **27**, 1739–1740.
  46. Subramanian, A., Tamayo, P., Mootha, V.K., Mukherjee, S., Ebert, B.L., Gillette, M.A., Paulovich, A., Pomeroy, S.L., Golub, T.R., Lander, E.S., and Mesirov, J.P. (2005). Gene set enrichment analysis: A knowledge-based approach for interpreting genome-wide expression profiles. *Proc. Natl. Acad. Sci. USA* **102**, 15545–15550.

## STAR★METHODS

### KEY RESOURCES TABLE

REAGENT or RESOURCE	SOURCE	IDENTIFIER
<b>Antibodies</b>		
Living Colors	Takara	RRID: 632380
L-plastin	GeneTex	RRID: GTX124420
gH2AX phosphoSer139	GeneTex	RRID: GTX127342
Cleaved Caspase-3	Abcam	RRID: ab13847
PCNA	Abcam	RRID: sc7907
L-plastin	GeneTex	RRID: GTX124420
gH2AX phosphoSer139	GeneTex	RRID: GTX127342
Cleaved Caspase-3	Abcam	RRID: ab13847
PCNA	Abcam	RRID: sc7907
<b>Chemicals, peptides, and recombinant proteins</b>		
RSAI	ThermoFisher	RRID: ER1121
HINFI	ThermoFisher	RRID: ER0801
F29 DNA polymerase	Biolabs	RRID: M0269L
HotStart Taq Polymerase	Qiagen	RRID: 203205
HINFI	ThermoFisher	RRID: ER0801
F29 DNA polymerase	Biolabs	RRID: M0269L
HotStart Taq Polymerase	Qiagen	RRID: 203205
<b>Critical commercial assays</b>		
telomere PNA probe	Panagen	RRID: F1002
<b>Deposited data</b>		
RNA-seq data	National Center for Biotechnology Information (NCBI)	CNBI: PRJNA944150
DNA-seq data	European Nucleotide Archive (ENA)	ENA: PRJEB81410
<b>Experimental models: Cell lines</b>		
U2OS	ATCC	RRID: HTB-96
HeLa	ATCC	RRID: CCL-2
ZMEL	Provided by Richard White (University of Oxford)	–
<b>Experimental models: Organisms/strains</b>		
<i>tert</i> hu3430	ZFIN repository	ZDB-GENO-100412-50
Tg( <i>mitfa</i> :Hsa.HRAS_G12V, <i>mitfa</i> :GFP)	ZFIN repository	ZDB-TGCONSTRUCT-110127-2
PRKDC <sup>-/-</sup>	Imported from David M. Langenau's lab (Harvard University)	–
<i>mitfA</i> > BRAF(V600E)-Myc	Imported from Elizabeth Patton's lab (University of Edinburgh)	–
<b>Software and algorithms</b>		
ImageJ	National Institutes of Health	Version 2.9.0
GraphPad Prism	GraphPad software, LLC	Version 8.4.0
Internal pipeline for RNA-seq analysis	N/A	<a href="https://github.com/maliabird17/EI-Mai-GSEA-Analysis">https://github.com/maliabird17/EI-Mai-GSEA-Analysis</a>

### EXPERIMENTAL MODEL AND STUDY PARTICIPANT DETAILS

#### Ethics statement

All experiments involving animals have been approved in accordance with national animal welfare guidelines in France at the IRCAN zebrafish facility – PEMAV (authorization number #A06-088-24) in the context of the authorized animal experimentation projects

APAFIS#33396–2021112517136391 approved by the French Ministry and the local animal experimentation Ethical Committee - CIEPAL AZUR no. 28 and in Portugal by the Ethical Committee of the Instituto Gulbenkian de Ciência and approved by the competent Portuguese authority (Direcção Geral de Alimentação e Veterinária; approval number: 0421/000/000/2015).

### Zebrafish maintenance

Zebrafish were maintained in accordance with Institutional and National animal care protocols. The telomerase mutant zebrafish *tert*<sup>+<sup>hu343026</sup>/–</sup> (referred in this work as *tert*+/–) were crossed either with *Tg(mitfa:Hsa.HRAS\_G12V,mitfa:GFP)*<sup>27</sup> or *Tg(mitfa:BRAFV600E)*; *tp53*<sup>+<sup>M214K28</sup>/–</sup> to generate the stock melanoma lines containing the *tert* mutation. All *tert*+/– lines are maintained as outcross to *tert*+/+ to avoid the effects of haploinsufficiency in the progeny.<sup>43</sup> The experimental fish were obtained by crossing *tert*+/– fish with either *Tg(mitfa:Hsa.HRAS\_G12V,mitfa:GFP)*; *tert*+/– or *Tg(mitfa:BRAFV600E)*; *tp53*<sup>+<sup>M214K</sup>/–</sup>; *tert*+/– to ensure that HRAS+ and BRAF+ fish possessed a single copy of the oncogene. Finally, to generate immunocompromised zebrafish, we incrossed the *prkdc*<sup>+<sup>D3612fs</sup>/–</sup> line to generate *prkdc*<sup>–/–</sup> homozygous fish.

### Cell culture

For the telomerase activity assay and c-circle assay, HeLa, U2OS and ZMEL cell lines were used as positive and negative controls. These cell lines were cultured under standard cell culture conditions with DMEM supplemented with 10% FBS. These cell lines were not authenticated and they were not tested for mycoplasma. Nevertheless, they performed as expected for each assay.

## METHOD DETAILS

### Fixation for histology and immunofluorescence

The animals were euthanized with 1 g/L of MS222 and then fixed in 10% neutral buffered formalin for 72 h at room temperature. The fish were then decalcified in 0.5M EDTA for 48 h and the whole fish were embedded in paraffin. Transversal sections of 5µm were obtained, and the slides were stained with hematoxylin and eosin for histopathological analysis. Additionally, slides were used for immunofluorescence analysis.

### Immunofluorescence of paraffin embedded zebrafish

Paraffin-embedded sections were deparaffinized with HistoChoice clearing agent (H2779, Sigma-Aldrich) and rehydrated using a series of alcohols (100%, 80%, 60%). Slides were then placed in citrate buffer (10 mM, pH 6) and microwaved at 550W for 20 min. After cooling, slides were washed in PBS followed by incubation in blocking buffer (2% Normal Goat Serum, 1% DMSO, 0.1% tween in PBS) for 1 h at room temperature. Subsequently, slides were incubated overnight at 4°C with primary antibody diluted in blocking buffer (these were: 1:200 Living Colors Ab, #632380, Takara; 1:100 L-plastin, #GTX124420, GeneTex; 1:50 γH2AX phosphoSer139; #GTX127342; GeneTex; 1:50 Cleaved Caspase-3, #ab13847, Abcam; 1:50 PCNA, #sc7907, Santa Cruz). The following day, slides were washed 3 times with PBS and incubated with the secondary antibody (1:500) for 2 h at room temperature. This was followed by 3 washes with PBS and incubated with DAPI (1:2000 in dH2O) for 10 min. Finally, slides were washed with PBS for 10 min at room temperature and mounted with Fluoroshield (#F6182, Sigma). Stainings were imaged on Delta Vision Elite (GE Healthcare). Whole tumor area was identified by the GFP staining. Quantification of the different antibodies was performed by quantifying the percentage of positive cells within the tumor area for a minimum of 200 cells per slide.

### Sample collection

The fish with tumors were euthanized using 1 g/L of MS222, and the tumors and/or skin were dissected and rinsed with ice-cold PBS. Samples intended for molecular analysis were either used immediately or snap-frozen in liquid nitrogen and stored at –80°C. Tumor samples designated for allografts were utilized without further processing.

### Telomere restriction fragment (TRF) analysis by Southern blot

Tumor and skin samples were lysed overnight at 50°C in lysis buffer (#K0512, Fermentas) with 1 mg/mL Proteinase K and RNase A (1:100) and genomic DNA was extracted using a standard phenol-chloroform protocol. Genomic DNA was then digested with *RSAI* and *HINF*I enzymes for 12 h at 37°C. After digestion, samples were loaded on a 0.6% agarose gel in 0.5% TBE buffer. The gel was run at the constant voltage of 110V for at least 17 h at 4°C. Gels were then fixed with 0.25N HCl for 15 min and processed for Southern blotting using a 1.6 kb telomere probe, (TTAGGG)<sub>n</sub>, labeled with [ $\alpha$ -32P]-dCTP.

### C-circle assay

C-circle assay was carried on as described by Henson et al.<sup>44</sup> Briefly, 30ng of genomic DNA was used for each reaction containing 7.5 U  $\Phi$ 29 (#M0269L, BioLabs), 1x  $\Phi$ 29 DNA polymerase buffer, 0.2 mg/mL BSA, 0.1% (v/v) Tween 20, 1 mM each dATP, dTTP, dGTP, 4 µM dithiothreitol (DTT). The rolling circle amplification reaction proceeded as follow: 8 h at 30°C and 20 min at 65°C using a thermocycle machine. For each sample, a reaction without the  $\Phi$ 29 DNA polymerase was used as a control (- $\Phi$ 29). Using a 96-well Bio-Dot Apparatus (Bio- Rad), reaction products (1:8 dilution in 2x SCC) were dot-plotted onto a 2x SCC pre-soaked positive nylon

membrane. The membrane was then UV-crosslinked and hybridized with a 1.6 kb telomere probe, (TTAGGG)<sub>n</sub>, labeled with [ $\alpha$ -<sup>32</sup>P]-dCTP.

### TRAP assay

Tumor samples were homogenized in 0.5% CHAPS followed by incubation on ice for 30 min. Samples were then centrifuged (16000xg for 20 min at 4°C) and the supernatant was collected. Protein concentration was measured using a Bradford assay according to manufacturer's instructions. 0.5  $\mu$ g of whole protein was added to the TRAP master mix, which contained 1x HotStart Taq Polymerase (#203205, Qiagen), 1x TRAP buffer (20mM Tris-HCL pH 8.3, 1.5mM MgCl<sub>2</sub>, 63mM KCl, 0.05% (v/v) Tween 20 and 1mM EGTA), 25 $\mu$ M dNTPs, 0.8 ng/ $\mu$ L BSA and the following primers 100 ng/ $\mu$ L ACX: GCGCGCTTACCCTTACCCTTACCCTAACCC, 100 ng/ $\mu$ L NT: ATCGCTTCTCGGCCTTTT, 0.01 attomol/ $\mu$ L TSNT: AATCCGTCGAGCAGAGTTAAAAGGCCGAGAAGCGAT, 2 ng/ $\mu$ L TS: AATCCGTCGAGCAGAGTT. As negative control, samples were treated with 12.25 mg/ml Rnase for 20 min at 37°C. Reactions were then kept in the dark for 30 min at room temperature, followed by 15 min at 95°C, 30 cycles of 30 s at 95°C, 30s 52°C and 45 s at 72°C and a final step of 10 min at 72°C. TRAP products were run on a 10% polyacrylamide gel with 1x TBE.

### RNA extraction/RNA sequencing

RNA extraction was performed using a TRIzol-chloroform protocol according to manufacturer's specifications. RNA quality was assessed by BioAnalyzer (Agilent 2100). RNA-seq library preparations and sequencing were outsourced to Beijing Genomics Institute (BGI, Hongkong). Briefly, pair ended 150 bases reads were sequenced on DNBseq platform and 100M clean reads per sample was generated. The RNA-seq data was analyzed by an internal pipeline for transcript comparison. Before running, genes were mapped to zebrafish orthologs using Ensembl's Biomart database. Using MsigDB's Hallmark gene set,<sup>45,46</sup> the gene set enrichment analysis (GSEA) was run on the Broad Institute's GSEA Software. One thousand permutations were run with a gene set permutation type. Significant enrichment results ( $p \leq 0.05$ ) were considered to be GSEA hallmarks. Borderline significance (to show directionality) was set at nominal  $p$ -values below 0.05 and false discovery rate below 0.25.

### Tumor allografts

Tumor samples were dissociated with TryPLE (ThermoFisher Scientific) for 20 min at 30°C and filtered using a 70 $\mu$ m cell strainer (#22363538, Fisher Scientific). Cells were then stained with Trypan Blue and counted with a hemocytometer and diluted in PBS to a final concentration of 100 000 cells/ $\mu$ L. Immunocompromised zebrafish (*prkdc*<sup>-/-</sup>) were anesthetized with 160  $\mu$ g/L MS222 and injected subcutaneously with ca. 500 000 cells on the left flank below the dorsal fin. After the procedure, fish were placed back into tanks containing system water and their recovery was monitored until they regained normal swimming pattern. Injected fish were imaged using a fluorescence stereomicroscope (Leica M205FA) at 1- and 2-month post injection.

### Telomere dysfunction-induced focus (TIF)

The tumors were excised and dissected to small pieces. They were then transferred to a solution of 1.1% sodium citrate and left at room temperature for 8 min, followed by an additional 8 min on ice. After this, the samples were transferred to a 3:1 solution of methanol and acetic acid. The solution was replaced after 20 min, and the samples were kept overnight at -20°C. The following day, the samples were transferred to a 50% acetic acid solution, the tissue was dissociated with a blade, and the cells were filtered through a 70 $\mu$ m cell strainer (#22363538, Fisher Scientific). The cells were then deposited onto a slide using a cytospin centrifuge and allowed to air-dry. The cells were permeabilized with 0.5% Triton X-100 for 8 min and dehydrated with a series of ethanol. Next, hybridization of the telomere PNA probe (#F1002, Panagen) was performed for 2 h at room temperature after denaturation in a solution of 10mM Tris-HCl pH 7.2, 70% formamide, and 1% blocking solution (#11096176001, Roche) for 3 min at 85°C. The cells were then washed for 30 min with 10mM Tris-HCl pH 7.2, 70% formamide, followed by a second wash with 50mM Tris-HCl pH 7.5, 150 mM NaCl for 15 min. The cells were then incubated with a blocking buffer (1% Triton X-100, 1% BSA, 5% normal goat serum) for 1 h, followed by primary antibody incubation (1:50  $\gamma$ H2AX phospho Ser139; #GTX127342; GeneTex) overnight at 4°C. The cells were then washed with PBS, followed by secondary antibody incubation for 2 h at room temperature and 10 min of DAPI incubation (1:2000 in dH<sub>2</sub>O). Finally, the slides were mounted with FluoroshieldTM (#F6182, Sigma), and the staining was imaged on a Delta Vision Elite (GE Healthcare). The number of  $\gamma$ H2AX foci colocalizing to telomeres was quantified per nucleus. A minimum of 100 nuclei were assessed per group.

## QUANTIFICATION AND STATISTICAL ANALYSIS

### Tumor size quantification

Fish were anesthetized with 160  $\mu$ g/L of tricaine methane sulfonate solution (MS222), placed on a 1% agarose-coated Petri dish and immediately imaged using a fluorescence stereomicroscope (Leica M205FA). After the procedure, fish were placed back in tanks containing system water and monitored for recovery until they regained a normal swimming pattern. Images were analyzed by the software ImageJ (version 2.9.0). We outlined the tumor and quantified its area by considering both the GFP signal and visible outgrowth on the skin. To determine tumor growth, we generated a linear regression of the area at different timepoints and obtained a slope to represent progression.

**Statistical analysis**

Statistical analysis and graphs were done in GraphPad Prism 8.4.0 software. Student's t-test was used to compare the mean of 2 experimental groups and One-Way ANOVA was used to compare the mean of 3 or more experimental groups with normally distributed data. Chi-square test was used to compare 2 or more groups of discrete data. The specific statistical test used for each graph and other statistical details are described in the corresponding figure legend. A  $p \leq 0.05$  was considered significant throughout of the study and the exact  $p$  values are present in the text of the result's section.

**ADDITIONAL RESOURCES**

No additional resources were used in this study.